

Estimation of multicomponent signals by using time-frequency representations with application to knock signal analysis

Igor Djurović, Mark Urlaub, Johann F. Böhme, LJubiša Stanković

Abstract—Time-frequency representation based estimation of multicomponent signal parameters is considered. A new adaptive threshold combined with a pattern recognition tool is proposed to separate signal components from the mixture. The proposed algorithm is applied to knock signal analysis in spark ignition engines.

I. INTRODUCTION

Knock of combustions can lead to serious problems in spark ignition car engines, e.g., environment pollution, mechanical damages, and reduced energy efficiency. Careful spark ignition control prevents the engine from frequent knock. The main issue in knock signal analysis is knock detection, but detailed knowledge of knock parameters including those of in-cylinder pressure and structure-borne sound can also be important. An interesting topic based on knock signal analysis is the optimal positioning of piezoelectric devices used for vibrations recording. Methods for knock detection are reviewed in [1]. We will focus on the analysis of pressure and vibration signals caused by knock. Resonance frequencies determined by piston position, in-cylinder temperature and velocity of sound in the combustion chamber were investigated by using the finite element method in [2]. High pass filtered pressure and vibration signals in the case of knock can be assumed as multicomponent FM signals. In this paper, parameters of the components will be estimated by using time-frequency representations (TFR). An adaptive threshold is applied to the TFR in order to separate signal components. Several other papers also deal with TFR based methods in knock signal analysis [3], [4]. The

EUSIPCO 2004.

Wigner distribution (WD) and the S-method (SM) are used to estimate knock signal parameters in [5], [6]. For precise parameter estimation, several combustion processes are averaged and positions of resonance frequencies are estimated from resulting TFR. An analysis of combustion parameters based on a single signal observation is described in [7]. The so-called “peeling method” for parameter estimation from the multicomponent signal is applied. But this method can be inaccurate for signals with varying amplitude or in a noisy environment or if the distance between components is varying. In this paper an adaptive threshold is applied for the determination of the signal component positions in the TF plane. The fact that TFRs are highly concentrated around the instantaneous frequency (IF) is used for threshold determination. An additional criterion is applied to remove components caused by noise or interferences. Signal components are separated in the TF plane by using the modified grass-fire algorithm [8]. The IFs of the signal components are estimated based on the maxima positions or the moments of the TF component. Other parameters as amplitude and initial phase are estimated in a straightforward manner. The algorithm is tested by simulated and real-life signals. Note that the proposed algorithm does not assume any knowledge of signal support regions in advance.

II. SIGNAL MODEL AND REGION OF INTEREST

Consider a multicomponent signal $x(t) = \sum_{i=1}^P x_i(t) + \nu(t)$ where $x_i(t) = A_i(t) \exp(j\phi_i(t))$, for $t_i > t$ (t_i is the signal component appearance instant). Assume that

$|dA_i(t)/dt| \ll |d\phi_i(t)/dt|$ for $i = 1, \dots, P$ and $\forall t$ (amplitudes are slow-varying compared to phases), and $\phi_i'(t) \neq \phi_j'(t)$ for $\forall t$ (IFs are non-intersecting functions). The TFR of this signal can be written as

$$TF_x(t, \omega) \approx \sum_{i=1}^P TF_{x_i}(t, \omega) + Q(t, \omega),$$

where $Q(t, \omega)$ is caused by noise and (cross-)interferences between signal and noise components. Assume that, in the used TFR, $Q(t, \omega)$ can be neglected and that signal components are highly concentrated along the IF, $TF_{x_i}(t, \omega) \approx 2\pi A_i^2(t)\delta(\omega - \phi_i'(t))$. We will use the SM as the TFR [9]:

$$SM(t, \omega) = |STFT(t, \omega)|^2 + 2\Re \left[\sum_{l=1}^L STFT(t, \omega + l\Delta\omega) \times STFT^*(t, \omega - l\Delta\omega) \right],$$

where $\Delta\omega$ is the frequency step and $STFT(t, \omega)$ is the short-time Fourier transform (STFT):

$$STFT(t, \omega) = STFT(n\Delta t, k\Delta\omega) = \sum_{m=-N/2}^{N/2-1} x((n+m)\Delta t)w(m\Delta t) \times \exp(-jkm\Delta\omega\Delta t)$$

where Δt is sampling rate. The SM can be highly concentrated on the IFs of the signal components while avoiding interferences between signal components for appropriate L . The selection of parameter L is discussed in [10].

The first step in our procedure is to recognize the region of the signal components in the TF plane. This is denoted as $R(t, \omega)$, where $R(t, \omega) = 1$ means that point (t, ω) belongs to the signal components, while $R(t, \omega) = 0$ means that (t, ω) is outside of signal components. The function $R(t, \omega)$ known as the region-of-interest in pattern recognition terminology and indicating the existence of the

signal components is determined based on an adaptive threshold as

$$R(t, \omega) = 1 \text{ if } \frac{\sum_{\mathbf{A}_{t\omega}} TF_x(\tau, \theta)}{\sum_{\mathbf{B}_{t\omega}} TF_x(\tau, \theta)} \geq p$$

$$\text{and } TF_x(\tau, \theta) \geq \max[qm_x(t), r\gamma_x], \quad (1)$$

and $= 0$ elsewhere, where $\mathbf{A}_{t\omega}$ and $\mathbf{B}_{t\omega}$ are narrow and wide regions centered around the considered point (t, ω) . In simulations $m_x(t)$ is the maximum of the TFR in the considered instant $m_x(t) = \max_{\theta} TF_x(t, \theta)$, while γ_x is the maximum of the TFR in the entire plane $\gamma_x = \max_{\tau, \theta} TF_x(\tau, \theta)$. Reasons for selection of criteria in are: (a) If (t, ω) is an IF point then the ratio between signal energy in the narrow and the wide regions around the considered point is high, otherwise, this ratio is significantly smaller. (b) Some relatively weak components but with large magnitudes compared to the neighbor points could be recognized as a signal. Two additional criteria are introduced in (1) to avoid this problem. The first removes all components with a smaller amplitude than the preassigned percentage of the TFR maximum in the considered instant and the other removes points with a weak TFR.

Selection of the parameters in (1). Rectangular shaped regions $\mathbf{A}_{t\omega}$ and $\mathbf{B}_{t\omega}$ are considered: $\mathbf{A}_{t\omega} = [t - T_A\Delta t, t + T_A\Delta t] \times [\omega - \Omega_A\Delta\omega, \omega + \Omega_A\Delta\omega]$ with a size of $(2T_A + 1) \times (2\Omega_A + 1)$ TF points and $\mathbf{B}_{t\omega} = [t - T_B\Delta t, t + T_B\Delta t] \times [\omega - \Omega_B\Delta\omega, \omega + \Omega_B\Delta\omega]$ with a size of $(2T_B + 1) \times (2\Omega_B + 1)$ TF points. Assume that the TF components are well separated, i.e., for more than $(2\Omega_B + 1)\Delta\omega$ along the frequency axis and that the TFR of the considered signal component is concentrated in a single point at each instant exactly on the IF. Let the value on IF be Θ , while the average value of the TFR outside of the signal component be ε , and $\Theta \gg \varepsilon$. Then the ratio $\sum_{\mathbf{A}_{t\omega}} TF_x(\tau, \theta) / \sum_{\mathbf{B}_{t\omega}} TF_x(\tau, \theta)$ is approximately equal to $(2T_A + 1)/(2T_B + 1)$ if (t, ω) is on the IF while it is $(2T_A + 1)(2\Omega_A + 1)/(2T_B + 1)(2\Omega_B + 1)$ if (t, ω) is outside the IF. Thus, the parameter p should satisfy,

$$\frac{(2T_A+1)(2\Omega_A+1)}{(2T_B+1)(2\Omega_B+1)} < p < \frac{2T_A+1}{2T_B+1}.$$

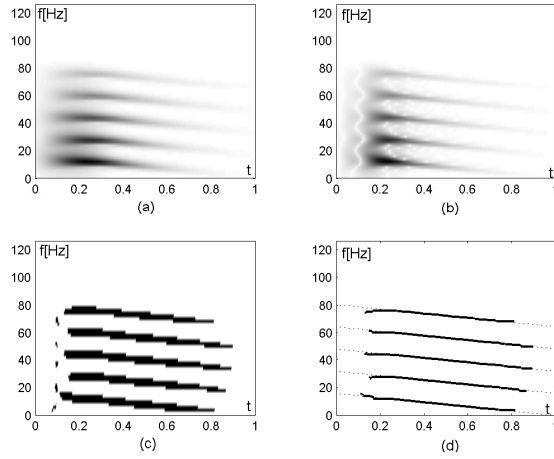


Fig. 1. TFRs and component segmentation for the synthetic signal: (a) SPECT; (b) SM; (c) $R(t, \omega)$; (d) IF estimation (dotted lines exact IF; solid line - estimates).

It can be seen that $T_A \leq T_B$ and $\Omega_A < \Omega_B$. The IF of combustion signals in this application is relatively slow varying, see Section IV. Therefore, we selected $T_A = T_B = 20$. Results generally do not vary significantly for different T_A and T_B . For signals with fast variations in the IF, T_A and T_B should be small. Since our goal is the separation of close signal components, values Ω_A and Ω_B should be chosen as small as possible. In simulations, $\Omega_A = 1$ and $\Omega_B = 3$ are set. Thus, parameter p should be selected within $3/7 < p < 1$. We selected p close to the lower bound, $p = 0.5$, since the considered signals are non-noisy and it is required to keep relatively weak components. In higher noise environments the parameter p should be greater than in this application.

The other criterion in (1) is introduced to remove TF regions, influenced by noise or by interferences, satisfying the first criterion. In order to keep weak signal components, very small values for q and r should be adopted. Values $q = 1.5\%$ and $r = 0.1\%$ are used in simulations, where similar results are obtained with any $q < 2\%$ and $r < 1\%$.

III. SIGNAL COMPONENTS SEPARATION

The grass-fire algorithm used in the pattern recognition [8] for components separation from a binary image $R(t, \omega)$ has been applied. The search for the first point $R(t_0, \omega_0) = 1$ (grass

phase) is performed. All points $R(\tau, \theta) = 1$ such that there is a path between (τ, θ) and (t_0, ω_0) passing through the points that belong to $R(t, \omega) = 1$ (fire phase) are assigned to the particular signal component. The selected component is removed from the binary image $R(t, \omega)$ and the search is repeated for a new “grass” point. The algorithm stops when no “grass” points exist anymore. The $R(t, \omega)$ can be written as: $R(t, \omega) = \max_{i=1, \dots, T} R_i(t, \omega)$, where $R_i(t, \omega)$ are regions of detected components; T is the number of separated parts of $R(t, \omega)$. Assume that signal regions are ordered in such a way that region $R_i(t, \omega)$ contains higher energy than $R_{i+1}(t, \omega)$. We will neglect all components with small energy compared to the entire signal energy. It means $\Omega(t, \omega) = \max_{j>\rho} R_j(t, \omega)$, will not be considered since signal energy in the region $R_j(t, \omega)$, $j > \rho$, is small, $\sum_{R_j(t, \omega)} TF_x(\tau, \theta) \ll \sum_{\forall(t, \omega)} TF_x(\tau, \theta)$. Alternative criterion for selecting the number of signal components can be obtained by using the fact that ρ should be equal to P if the number of signal components is known in advance. For example, it could be known that a considered engine produces specific resonance frequencies in the case of knock. In our simulation all regions producing less than 1% of the signal energy are removed from the analysis. The aim of

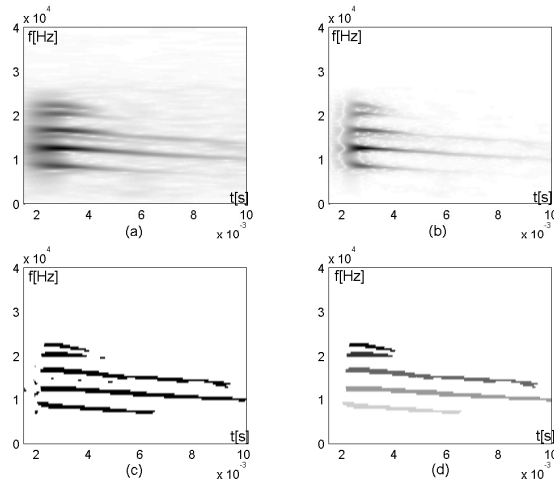


Fig. 2. TFRs and component segmentation for knock pressure signal: (a) SPEC; (b) SM; (c) $R(t, \omega)$; (d) Segmented components depicted in various gray scales.

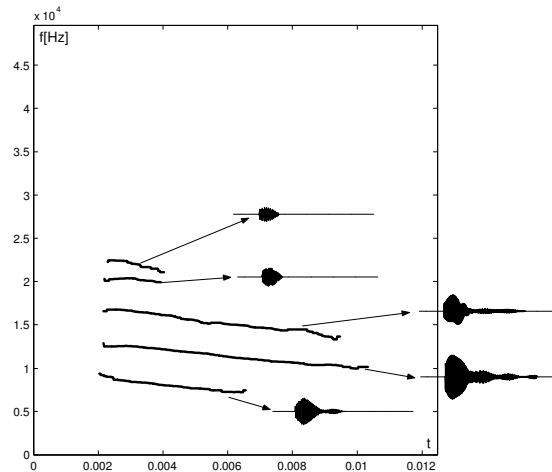


Fig. 3. IF estimates of signal components with reconstruction of the signal components.

this criterion is similar to the second criterion in (1) and it can be used to further relaxed choice of parameter q and r . Signal parameters can be estimated from signal regions $R_i(t, \omega)$, $i = 1, \dots, \rho$ as follows: 1. The IF can be estimated based on the maxima of $\hat{\omega}_i(t) = \arg \max_{\omega} TF_x(t, \omega) R_i(t, \omega)$, for $t \in [t_{ib}, t_{ie}]$, (t_{ib} and t_{ie} are estimated instants of the knock component appearance and disappearance). In order to refine the estimate, the frequency moment of the TFR could be used, $\hat{\omega}_i(t) = \sum_{\omega} \omega TF_x(t, \omega) R_i(t, \omega) / \sum_{\omega} TF_x(t, \omega) R_i(t, \omega)$.

The frequency moment can be used here since the amount of noise in this application is small. 2. The signal phase (up to ambiguity in the initial phase) can be estimated as $\hat{\phi}_i(t) = \int_{t_{ib}}^{t_{ie}} \hat{\omega}_i(t) dt$; 3. The signal can be dechirped as $\hat{y}_i(t) = x_i(t) \exp(-j\hat{\phi}_i(t))$, for $t \in [t_{ib}, t_{ie}]$ and $\hat{y}_i(t) = 0$ elsewhere. Amplitude and initial phase ($\hat{A}_i(t)$, $\hat{\phi}_i(t)$) can be extracted by low-pass filtering of $\hat{y}_i(t)$ using a classical setup.

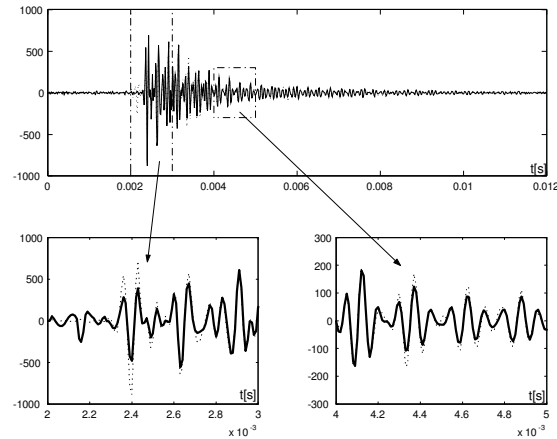


Fig. 4. Reconstruction of combustion knock signal: original signal - dotted line, reconstructed signal - solid line. Two zones from upper graph are magnified below.

TABLE I

NORMALIZED COVARIANCE BETWEEN ORIGINAL AND RECONSTRUCTED SIGNALS IN 50 TRIALS. MIN - MINIMAL COVARIANCE; MAX - MAXIMAL COVARIANCE; MEAN - AVERAGE COVARIANCE; <0.85 - NUMBER OF TRIALS WITH COVARIANCE LESS THAN 0.85.

Norm. covariance		min	max	mean	<0.85
1200rev/min	pres	0.8270	0.9446	0.9080	1
	vibr	0.8092	0.9215	0.8787	4
1750rev/min	pres	0.8694	0.9501	0.9132	0
	vibr	0.8267	0.9319	0.8754	6
2000rev/min	pres	0.8191	0.9366	0.8976	2
	vibr	0.8303	0.9160	0.8819	4
3000rev/min	pres	0.8410	0.9487	0.9078	1
	vibr	0.8356	0.9394	0.8992	1
3500rev/min	pres	0.8382	0.9548	0.9193	2
	vibr	0.8658	0.9457	0.9111	0

IV. EXAMPLES

Simulated signal. In order to illustrate the accuracy of the proposed method we considered sum of five signal components:

$$x(t) = \sum_{i=1}^5 A_i u(t - t_0) \times$$

$$\exp(-\alpha_i |t - t_0| - jat^2/2 + jb_i t)$$

where $u(t) = 1$ for $t > 0$ and $u(t) = 0$ elsewhere, and $A_i = 0.5 + i0.1$, $\alpha_i = 0.6 + 3i$, $a = 32\pi$, $t_0 = 0.1$, and $b_i = (6 - i)32\pi$, $i = 1, \dots, 5$. The considered interval is $t \in [0, 1]$. The sampling rate is $\Delta t = 1/512$. The spectrogram (SPEC) of this signal ($SPEC(t, \omega) =$

$|STFT(t, \omega)|^2$) using a Hanning window of width $N = 256$ is depicted in Fig.1a. It can be seen that components are spread in the TF plane. The SM ($L = 1$) is better concentrated, Fig.1b. The proposed algorithm is applied to the SM (parameters $p = 0.5$, $q = 1.5\%$ and $r = 0.1\%$) and the region $R(t, \omega)$ is depicted in Fig.1c. The estimated IF of the signal components are given in Fig.1d. Exact IFs of the signal components $\omega_i(t) = at - bi$, $i = 1, \dots, 5$, are represented with dotted lines. High accuracy can be seen in this case. From this simulation it can be concluded that the algorithm gives an accurate estimation of the time-

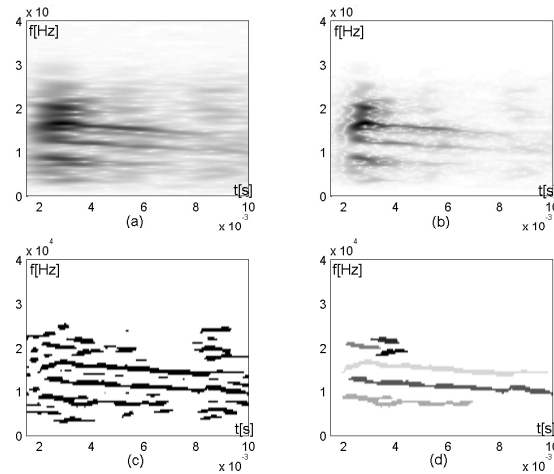


Fig. 5. TFRs and component segmentation for noisy knock vibration signal: (a) SPEC; (b) SM; (c) $R(t, \omega)$; (d) Segmented components depicted in various colors.

varying signal component parameters.

Knock signals. We consider a knock pressure signal recorded from a VW Passat engine at 1200 rpm. Note that the signal is high-pass filtered with a cut-off frequency of 3000 Hz. The sampling rate is $\Delta t = 10^{-2}$ ms and the signal contains 1280 samples. The SPEC and the SM with the same window as in the previous example are shown in Fig.2a,b. Parameter L in the SM is selected to be small ($L = 1$) to avoid interferences between close signal components. The algorithm with the same parameters as in the previous example is applied to the signal and $R(t, \omega)$ is depicted in Fig.2c. The grass-fire algorithm is applied to the binary image $R(t, \omega)$ and components with small energy (less than 1% of the signal energy) are removed, Fig.2d. The IF estimates are given in Fig.3. Reconstructed signal components are shown in the same figure. A signal reconstruction is shown in Fig.4 with two focused segments, where the original and the reconstructed signal are given for comparison. The algorithm is tested on 50 pressure and vibration signals recorded at 1200, 1750, 2000, 3000 and 3500 rpm. Results are summarized in Table 1. As a quality measure of the algorithm, the correlation coefficient between the original and the reconstructed signal is considered. The average of the correlation coefficient is above 0.85 (Table 1). The

worst result (0.8092) is achieved for the 31-st vibration signal recorded at 1200 rpm. The TFRs and signal regions are shown in Fig.5. It can be seen that the signal contains more noise than the previous one and the algorithm with parameters selected for a non-noisy signal case produces numerous components in the $R(t, \omega)$, see Fig.5c. However, after elimination of the regions producing small energy we obtained accurate estimates of the signal components, Fig.5d. Here, a small correlation coefficient means that we eliminated some noise influenced components by the proposed approach and that a small correlation coefficient is expected in this case

V. CONCLUSION

An algorithm for adaptive selection of signal component regions in the TF plane is proposed and applied to knock signal estimation. The selection of the algorithm parameters is discussed. The algorithm is tested on simulated and real-life signals. The performance of the algorithm is measured by using the correlation coefficient between the original and the reconstructed signal. The experimental results are promising.

REFERENCES

- [1] O. Boubal: "Knock detection in automotive engines," *IEEE Inst. Meas. Mag.*, Vol. 3, No. 3,

- 2000, pp. 24-28.
- [2] S. Carstens-Behrens, M. Urlaub, J. F. Böhme, J. Forster, F. Raichle: "FEM approximation of internal combustion chambers for knock investigation", *Society of Automotive Engineers*, 2002, paper no. 01-0237.
- [3] F. Molinaro, F. Castanie: "A comparison of time-frequency models", *Proc. EUSIPCO*, Barcelona, 1990, pp. 145-148.
- [4] G. Matz, F. Hlawatsch: "Time-frequency subspace detectors and application to knock detection", *Int. J. Electron. Commun. (AEÜ)*, Vol. 53, No. 6, 1999, pp. 379-385.
- [5] S. Carstens-Behrens, J. F. Böhme: "Applying time-frequency methods to pressure and structure-borne sound for combustion diagnosis," in *Proc. of ISSPA 2001*, Vol.1, pp.256-259, Aug.2001.
- [6] D. König, J. F. Böhme: "Application of cyclostationary and time-frequency signal analysis to car engine diagnosis," in *Proc. of ICASSP 1994*, Vol.4, pp.149-152, Apr. 1994.
- [7] L.J. Stanković, J. F. Böhme: "Time-frequency analysis of multiple resonances in combustion engine signals," *Sig. Proc.*, Vol. 79, No. 1, pp.15-28, Nov. 1999.
- [8] I. Pitas: *Digital image processing algorithms*, Prentice Hall, 1993.
- [9] L.J. Stanković: "A method for time-frequency signal analysis," *IEEE Trans. SP*, Vol. 42, Jan. 1994, pp. 225-229.
- [10] L.J. Stanković: "An analysis of some time-frequency and time-scale distributions," *Ann. Telec.*, Vol. 49, No. 9-10, Sep./Oct. 1994, pp. 505-517.